Sains Malaysiana 52(10)(2023): 2907-2918
http://doi.org/10.17576/jsm-2023-5210-13

Characterization, Antibacterial and Toxicity Evaluation of Biosynthesized Zinc Oxide Nanoparticles utilizing *Eleuthrine bulbosa* Bulb Extract

(Pencirian, Penilaian Antibakteria dan Ketoksikan bagi Zarah Nano Zink Oksida Biosintesis menggunakan Ekstrak Bebawang *Eleuthrine bulbosa*)

NORAZALINA SAAD*, CHE AZURAHANIM CHE ABDULLAH, NURUL ATHIKAH ADILA ZAINAL & EMMELLIE LAURA ALBERT

Department of Physics, Faculty of Science, Universiti Putra Malaysia, 43400 UPM Serdang, Selangor, Malaysia

Received: 2 May 2023/Accepted: 15 October 2023

ABSTRACT

In the current study, *Eleuthrine bulbosa* bulb extract was utilized to synthesize zinc oxide nanoparticles (ZnO NPs) in a simple, sustainable, and environmentally friendly manner. The bioactive compounds of *E. bulbosa* extract were identified by gas chromatography-mass spectrometry (GC-MS). Following synthesis of the ZnO NPs via the green method with *E. bulbosa* bulb extract as the reducing and capping agent, ZnO NPs were characterized using X-Ray Diffraction (XRD), Fourier Transform Infrared Spectroscopy (FTIR), Ultraviolet-Visible Spectroscopy (UV-Vis), and Photoluminescence (PL) further evaluated for antibacterial and cytotoxic activities. GC-MS analysis showed the presence of phytochemical compounds acting as reducing and capping agents. The UV-Vis spectra of ZnO nanoparticles containing *E. bulbosa* extract showed an optical energy bandgap between 3.12 and 3.89 eV. In addition, XRD showed that the crystalline size of ZnO NPs ranged from 21 to 68 nm with a wurtzite crystal structure. FTIR analysis showed that the plant extract contains identified functional groups including alcohols, phenols, alkene, and flavonoid compounds that influenced the mechanism of bonding with ZnO NPs. Particularly, the peaks of formation of Zn-O stretching vibrations at 470 to 480 cm^{-1} were successfully shown. In addition, ZnO NPs displayed antibacterial activity, which was greatest against *Staphylococcus aureus*, and were cytotoxic to MCF-7 and MCF-10A breast cells with IC_{50} values of 5.540 µg/mL and 15.77 µg/mL, respectively. ZnO NPs were successfully synthesized utilizing a green method, resulting in intriguing biocompatible potential candidates for use in both biomedical and environmental fields due to their eco-friendly synthesis and nontoxic.

Keywords: *Eleuthrine bulbosa; Staphylococcus aureus*; zinc oxide nanoparticles

ABSTRAK

Dalam kajian ini, ekstrak *Eleuthrine bulbosa* digunakan buat kali pertama untuk mensintesis nanozarah zink oksida (NPs ZnO) dengan cara yang mudah, mampan dan mesra alam. Sebatian bioaktif ekstrak *E. bulbosa* telah dikenal pasti oleh kromatografi gas-spektrometri jisim (GC-MS). Berikutan sintesis NP ZnO melalui kaedah pengekstrakan hijau *E. bulbosa* sebagai agen penurunan dan pengekapan, NP ZnO yang disintesis telah dicirikan menggunakan Pembelauan Sinar-X (XRD), Spektroskopi Inframerah Transformasi Fourier (FTIR), Spektroskopi Ultralembayung-Nampak (UV-Vis) dan *Photoluminescence* (PL) seterusnya dinilai untuk aktiviti antibakteria dan sitotoksik. Analisis GC-MS mendedahkan kehadiran sebatian fitokimia yang bertindak sebagai agen penurunan dan pengekapan. Spektrum UV-Vis nanozarah ZnO yang mengandungi ekstrak *E. bulbosa* mendedahkan jurang jalur tenaga optik antara 3.12 dan 3.89 eV. Di samping itu, XRD mendedahkan bahawa saiz kristal ZnO NPs antara 21 hingga 68 nm dengan struktur kristal wurtzite. Analisis FTIR menunjukkan bahawa ekstrak tumbuhan mengandungi kumpulan berfungsi termasuk kumpulan alkohol, fenol, alkena dan flavonoid yang dikenal pasti menyumbang kepada mekanisme ikatan dengan NP ZnO. Secara khususnya, puncak pembentukan getaran regangan Zn-O pada 470 hingga 480 cm^{-1} berjaya dilihat. Di samping itu, NP ZnO menunjukkan aktiviti antibakteria, yang paling besar terhadap *Staphylococcus aureus* dan sitotoksik kepada sel payudara MCF-7 dan MCF-10A dengan nilai IC_{50} masing-masing 5.540 µg/mL dan 15.77 µg/mL. NP ZnO berjaya disintesis menggunakan kaedah hijau, menghasilkan nanozarah ZnO berpotensi sebagai bioserasi yang menarik untuk aplikasi bioperubatan dan alam sekitar kerana sintesis mesra alam dan tidak toksik.

Kata kunci: *Eleuthrine bulbosa;* nanozarah zink oksida; *Staphylococcus aureus*

Introduction

Nanoparticles are influential in multiple disciplines including material science, medicine, engineering, and pharmacy in the field of nanotechnology. Among these nanoparticles, metal oxides, such as zinc oxide (ZnO), ferrosoferric oxide (Fe_3O_4), cadmium oxide (CdO), and copper oxide (CuO) have been utilized extensively as biological agents (Soto-Robles et al. 2019; Theophil Anand et al. 2019). Zinc oxide nanoparticles (ZnO NPs) have attracted the attention of researchers due to their unique chemical and optical characteristics that allow for modifications in their shape (Bala et al. 2015). With its appearance as a white powder and insoluble in water, ZnO has garnered considerable research attention for its characteristics of a broad bandgap to absorb and emit light as well as high exciton binding energies (Agarwal, Venkat Kumar & Rajeshkumar 2017; Selim et al. 2020; Siddiqi et al. 2018). Moreover, ZnO NPs are a highly suitable option for biological applications due to their high biocompatibility and facile synthesis process (Awwad et al. 2020).

Despite their potential benefits, the traditional approaches for producing ZnO nanoparticles using harmful reducing agents like hydrazine, dimethyl formamide (DMF), and sodium borohydride ($NaBH_4$) pose significant environmental risks (Hano & Abbasi 2022). To mitigate this issue, the green synthesis approach was introduced, which involves the synthesis of bioactive compounds with diverse molecular structures using sustainable raw materials like plants, fungi, bacteria, and algae, without the need for toxic chemicals (Anbuvannan et al. 2015; Bala et al. 2015).

The green synthesis of nanoparticles began by selecting an appropriate solvent and a 'green' substitute for the reducing agent. Biological reduction, which utilizes extracts of natural substances, is a secure and effective option that can serve as both reducing and capping agents, as well as stabilizers for the nanoparticles (Jain et al. 2021). These capping agents, such as proteins, enzymes, sugars, flavonoids, terpenoids, and cofactors, can be utilized to make the nanoparticle surface non-reactive. Hence, it will enhance the biocompatibility, stability, surface customization, controlled reactivity, environmental safety, dispersion, and adjustability of nanoparticles, while also reducing unintended interactions (Jain et al. 2021; Melkamu & Bitew 2021).

E. bulbosa, commonly known as Dayak onion, is an essential herbaceous plant that belongs to the Iridaceae family. It is extensively grown in various regions across Southern America, Africa, and Southeast Asia, where it is indigenous to Indonesia (Insanu et al. 2014; Kusuma et al. 2010). It exhibits a high concentration of flavonoids and phenols with antioxidant properties such as anthocyanin. Moreover, it contains constituents with anti-inflammatory, antibacterial, and antiviral effects, such as alkaloids, tannins, glycosides, and quinines (Kamarudin et al. 2020; Wicaksono et al. 2018). Since various bioactive components and biological properties of *E. bulbosa* have been reported, it might be a potential alternative as a good reducing agent for ZnO synthesis. However, the reducing ability of the *E. bulbosa* bulb has not been reported.

Hence, the aim of the current investigation was to employ a green approach to produce ZnO nanoparticles utilizing *E. bulbosa* extract as a reducing and capping agent. It also involved evaluating the structural, chemical, and optical characteristics of the synthesized nanoparticles, as well as investigating their potential antibacterial and cytotoxic effects on both non-cancerous and cancerous breast cells.

The reduction of metal oxides, such as ZnO, often involves the transfer of electrons from a reducing agent to the metal oxide, leading to the conversion of the metal oxide into its corresponding metal form. Potential bioactive chemicals that could contribute to the reduction of ZnO might include organic compounds with reducing properties, such as polyphenols, flavonoids, terpenoids, and alkaloids. These compounds are often found in plant extracts and can exhibit antioxidant and reducing activities.

Materials and Methods

Plant material, test organisms, chemicals, and reagents

Dayak onions were purchased from a nursery in Muar, Johor, Malaysia. The plant sample was identified and authenticated by the Biodiversity Unit, Institute of Bioscience, UPM Serdang, Selangor, Malaysia (Voucher specimen: MFI 0205/21). Gram-negative bacteria *Escherichia coli* (*E. coli*, ATCC 25922) and the Gram-positive bacterium *Staphylococcus aureus* (*S. aureus*, ATCC 43300) were acquired from the Microbial Culture Collection Unit (UNiCC), Institute of Bioscience, Universiti Putra Malaysia. Luria Bertani (LB) media and Luria Bertani (LB) agar was bought from Merck, Malaysia. MTT (3-(4,5-Dimethylthiazol-2-yl)-2,5-Diphenyltetrazolium Bromide) was purchased from Thermo Fisher Scientific. Dulbecco's Modified Eagle

Medium (DMEM), and Roswell Park Memorial Institute (RPMI) 1640 medium were bought from Nacalai Tesque. Fetal bovine serum (FBS) and penicillin-streptomycin antibiotics are bought from Capricorn Scientific.

PREPARATION OF *E. bulbosa* BULBS

The bulbs were peeled, thoroughly washed, sliced into 2-3 mm thick slices, and dried overnight at 40 °C. The dried bulbs were grounded into a powder, sieved using a 400 µm sieve, and kept at 4 °C for storage.

ETHANOLIC EXTRACTION AND LIQUID-LIQUID EXTRACTION

As referred to modified method by Kamarudin et al. (2020), the extraction of the bulbs was done using ethanol. Initially, 10 grams of powdered bulbs were mixed with 146 mL of 90% ethanol. Then, the mixture was heated for 70 min at 45 °C in a water bath. The resulting ethanol extract was filtered and concentrated using a rotary evaporator, and finally dried overnight at 40 °C.

Subsequently, the concentrated ethanol extract of *E. bulbosa* was fractionated into chloroform as organic solvents. First, the ethanol extract was dissolved in a 1:1 mixture of 95% ethanol and water. Next, n-hexane solvent was added to the mixture and partitioned using a separating funnel until it formed two layers. Then, chloroform solvent was added to the residue and repeated three times. The upper suspension layer was filtered and evaporated using a rotary evaporator before being dried at 40 °C overnight. The dried extracts were stored at -20 °C.

GC-MS ANALYSIS

The chloroform extract obtained was examined using gas chromatography-mass spectroscopy (GC-MS) for the identification of bioactive volatile compounds based on the mass chromatograms. GC-MS analysis of the samples was performed using Shimadzu GC-2010 Plus gas chromatography (Shimadzu Corporation, Japan). A low polarity column, RxiTM-5 ms fused silica capillary (30.0 m length × 0.25 mm internal diameter, 0.25 µm thickness), was used for the analysis. The gas chromatograph was set to split mode with a split ratio of 10.0 for injection. The initial column temperature was fixed at 50.0 °C, then increased to 300.0 °C at 3.00 °C/min. The constituents of the extract were identified by cross-referencing to published literature and comparing the mass spectra obtained with the following libraries: NIST11.lib, NIST11s.lib, FFNSC1.3.lib, and WILEY229.LIB. Each component was then relatively quantified based on the relative area of the peaks in the chromatogram.

BIOSYNTHESIS OF ZnO NPs

In this study, the synthesized ZnO NPs using 1, 3, and 6 mL of *E. bulbosa* extract were denoted as DO111, DO311, and DO611, respectively. First, 0.2 g of zinc acetate dihydrate ($Zn(CH_3CO_2)_2 \cdot 2H_2O$) was dissolved in 100 mL of distilled water. After that, different amounts (1, 3, and 6 mL) of *E. bulbosa* extract were added to the solution and stirred for two hours using a magnetic stirrer (Figure 1). While stirring, the pH adjustment was made to 11 using 2 M of NaOH for optimum condition of ZnO nanoparticles synthesis (Ribut et al. 2018). Then, the resulting mixture was placed in a centrifuge for 15 min at 6000 rpm. The solids that formed were washed twice with distilled water and ethanol to eliminate impurities. The solids were subsequently dried at a temperature of 60 °C for 24 h and subsequently, kept at room temperature for further analysis.

STRUCTURAL AND OPTICAL CHARACTERIZATION OF BIOSYNTHESIZED ZnONPs

To investigate the crystalline nature and formation of synthesized zinc oxide nanoparticles, a Ringaku X-ray diffractometer (UPM, Serdang, Malaysia) was employed with Copper K-α radiation at 40 kV and 15 mA and a scan rate of 10°/min. The sample was examined at 2θ ranging from 20° to 80° after being dried in the oven. The XRD patterns were analyzed using the X'pert Pro Highscore Plus software to identify the crystalline nature and phase purity of the sample. The functional groups of the nanoparticles were studied using Fourier Transform Infrared (FTIR) spectroscopy (Perkin-Elmer 1725X model) utilizing ATR technique in the range of 4000-400 cm^{-1}. Studies on luminescence were carried out at room temperature using a PerkinElmer LS 55 photoluminescence spectrometer with a Xenon (Xe) lamp as an exciting source. The Shimadzu Ultraviolet-Visible (UV-vis-NIR) Spectrophotometer (UV-3600) was used to measure the optical absorption spectra of ZnO nanoparticles in the wavelength range of 200-900 nm.

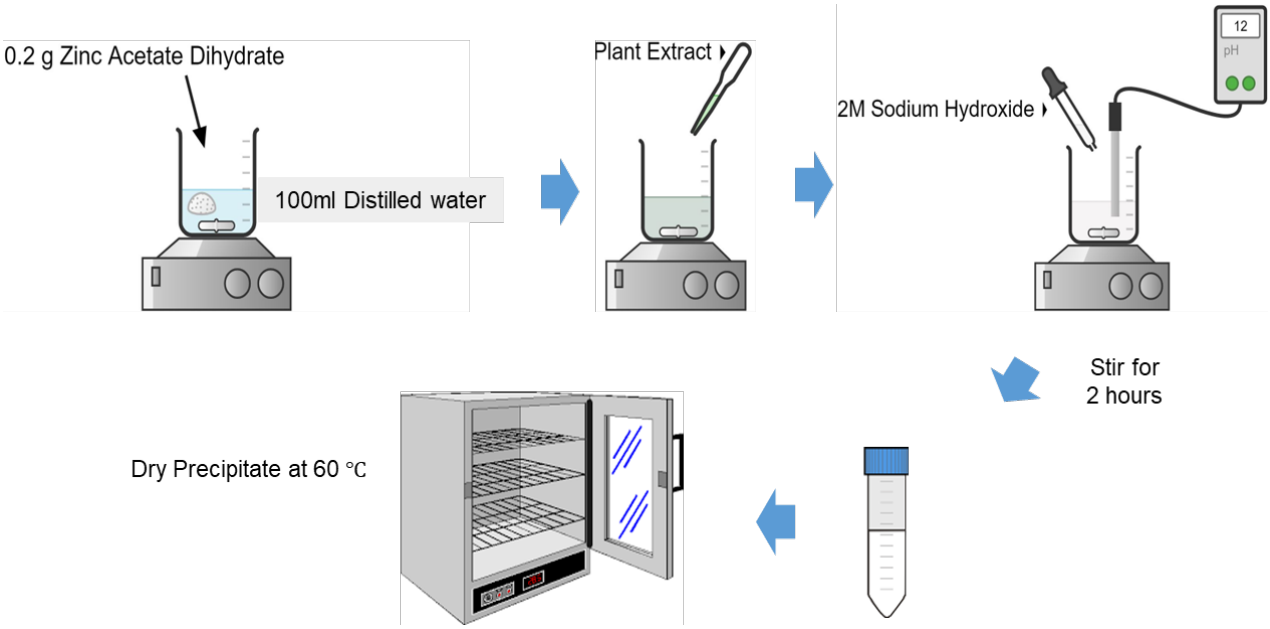

FIGURE 1. Synthesis of zinc oxide nanoparticles

ANTIMICROBIAL ACTIVITY

In this study, the antibacterial activity of *E. bulbosa* extract was evaluated using the disc diffusion method against the gram-positive bacteria *Staphylococcus aureus* (ATCC 43300) and the Gram-negative bacteria *Escherichia coli* (ATCC 25922). The method was adapted from Balouiri, Sadiki and Ibnsouda (2016) with slight modifications. Muller Hinton Agar (MHA) was made by pouring 15 mL of sterilized molten media into Petri dishes and allowing them to solidify for 5 min. A uniform swab of 0.1% inoculum suspension was dried for 5 min, and a 6 mm sterile disc was loaded with *E. bulbosa* extract at a concentration of 10 mg/mL. The MHA plates were incubated at 37 °C for 24 h after placing the loaded disc on their surface. The diameters of the inhibition zones that surrounded the discs were determined, and the experiment was carried out three times for accuracy. The bacterial strains were acquired from the Microbial Culture Collection Unit (UNiCC), Institute of Bioscience, Universiti Putra Malaysia.

In vitro CYTOTOXICITY EVALUATION OF ZnO NPs

CELL LINES AND REAGENTS

In this study, the human breast adenocarcinoma cell line MCF7 (ATCC® HTB-22TM) and human mammary epithelial cell line MCF-10A (CRL-10317™) were utilized. The cells were cultured in their respective complete growth media at 37 °C in a 5% CO_2 incubator from Thermo Fisher Scientific, USA. MCF7 cells were maintained in RPMI-1640 media supplemented with 10% (v/v) fetal bovine serum, 1% (v/v) penicillin/streptomycin, 20 ng/mL EGF, 0.5 mg/mL hydrocortisone and 10 µg/mL insulin. Meanwhile, MCF-10A cells were maintained in DMEM/F-12 media with 2% (v/v) horse serum, 1% (v/v) penicillin/streptomycin, 20 ng/mL EGF, 0.5 mg/mL hydrocortisone, and 10 µg/mL insulin. The cells were incubated under optimal conditions to ensure their growth and viability.

MTT ASSAY OF BIOSYNTHESIZED Zn ONPs

In order to assess the cytotoxicity of the synthesized ZnO NPs on MCF7 and MCF-10A cells, the MTT Assay was employed. The cells were initially seeded in 96-well plates at a density of 4×10^3 cells/mL and incubated overnight. The cells were then treated for 72 h at 37 °C with varied concentrations of ZnO NPs ranging from 1.56 µg/mL to 100 µg/mL. After the incubation period, MTT solution was added to the cells, followed by an additional 3-hour incubation period. The purple formazan crystals were then dissolved in DMSO, and the optical density of the samples was determined using an ELISA reader at 570 nm. Finally, cell viability was finally determined relative to the control groups using the following formula:

$$\text{Cell viability} = \frac{\text{Absorbance sample (mean)}}{\text{Absorbance control (mean)}} \times 100\%$$

The percentage of cell viability in relation to varying concentrations of ZnO NPs was graphed, following the methods of Van Tonder et al. (2015). The IC_{50} value, representing the concentration of treatment that resulted in a 50% reduction in cell viability, was calculated to determine cell viability inhibition. The experiment was conducted three times.

Results and Discussions

Identification of biological and chemical components in *E. bulbosa* extract using GCMS

GC–MS analysis was used to identify the component of *E. bulbosa* extract to prove the presence of capping agents and reducing agents in the plants. Based on the GC-MS spectra, phytochemical compounds present in *E. bulbosa* extract were identified based on their retention time (RT) consisting mainly propanoic acid, hexadecanoic acid, ethyl palmitate, coumarins, cis-12-octadecadienoic acid, benzeneethanal, 4-[1,1-dimethylethyl] and linoleic acid (Table 1). These chemical compounds could act as reducing and capping agents in ZnO NPs. A previous study by Agasti and Kaushik (2018) reported that stearic acid can be acted as capping agent and reducing agent which can protect nanoparticles from separation. In addition, the latest research by Liu et al. (2020) showed that Linoleic acid is also capable of reducing and capping agents. The electron-donating capacities, redox potentials, presence of functional groups (such as hydroxyl groups), and aromatic structures of alcohols, phenols, alkenes, and flavonoid compounds play important roles in the reducing and capping mechanisms of ZnO nanoparticle formation. These features determine their ability to reduce metal ions and stabilize ZnO nanoparticles, impacting the size, shape, and properties of the synthesized nanoparticles (Abomuti et al. 2021).

X-Ray DIFFRACTION (XRD) ANALYSIS OF ZnO NPs

X-ray diffraction (XRD) is employed for determining the crystal structure of materials and evaluating the size of crystalline domains present within the sample lattice. Figure 2 illustrates the XRD pattern of ZnO NPs denoted as DO111, DO311, and DO611. The XRD analysis shows that the ZnO NPs exhibit a crystalline nature corresponding to specific crystallographic planes, namely (100), (101), (102), (110), and (103), consistent with the hexagonal wurtzite structure of ZnO NPs. The JCPDS reference code 036-1451 confirms the aforementioned values and the wurtzite structure. Prior studies conducted by Pillai et al. (2020) and Ribut et al. (2018) have also reported analogous XRD patterns for green ZnO NPs.

TABLE 1. Identification of bioactive components in *E. bulbosa* chloroform extract based on GC-MS spectra

Peak	Compound name	Peak area %	Retention time	Molecular formula
1	Butane-2,3-diol	0.38	4.1663	$C_4H_{10}O_2$
2	2,3-Butanediol, [R-(R*,R*)]	0.47	4.3425	$C_4H_{10}O_2$
3	n-Hexadecanoic acid	1.49	50.8417	$C_{16}H_{32}O_2$
4	Ethyl palmitate	0.42	51.9708	$C_{18}H_{36}O_2$
5	Coumarine, 8-allyl-7-hydroxy-6-ethyl-4-methyl	2.36	55.4617	$C_{15}H_{16}O_3$
6	Linoleic acid	0.56	56.3982	$C_{18}H_{32}O_2$
7	Benzeneethanal, 4-[1,1-dimethylethyl]	0.78	56.8070	$C_{12}H_{16}O$
8	(R)-(-)-14-Methyl-8-hexadecyn-1-ol	1.02	57.3080	$C_{17}H_{32}O$
9	Eleutherine	-	59.4793	$C_{16}H_{16}O4$
10	Isoeleutherine	-	60.8885	$C_{16}H_{16}O4$
11	Propanedinitrile,[(3,4,5-trimethoxyphenyl) methylene]	20.92	64.8472	$C_{13}H_{12}N_2O_3$
12	Hexadecanoic acid, 2-hydroxy-1-(hydroxymethyl) ethyl ester	0.65	67.1923	$C_{19}H_{38}O_4$
16	Ethyl linoleate	0.97	71.8457	$C_{20}H_{36}O_2$
19	Stigmasterol	0.83	85.3685	$C_{29}H_{48}O$
20	Clionasterol	0.95	86.8377	$C_{29}H_{50}O$

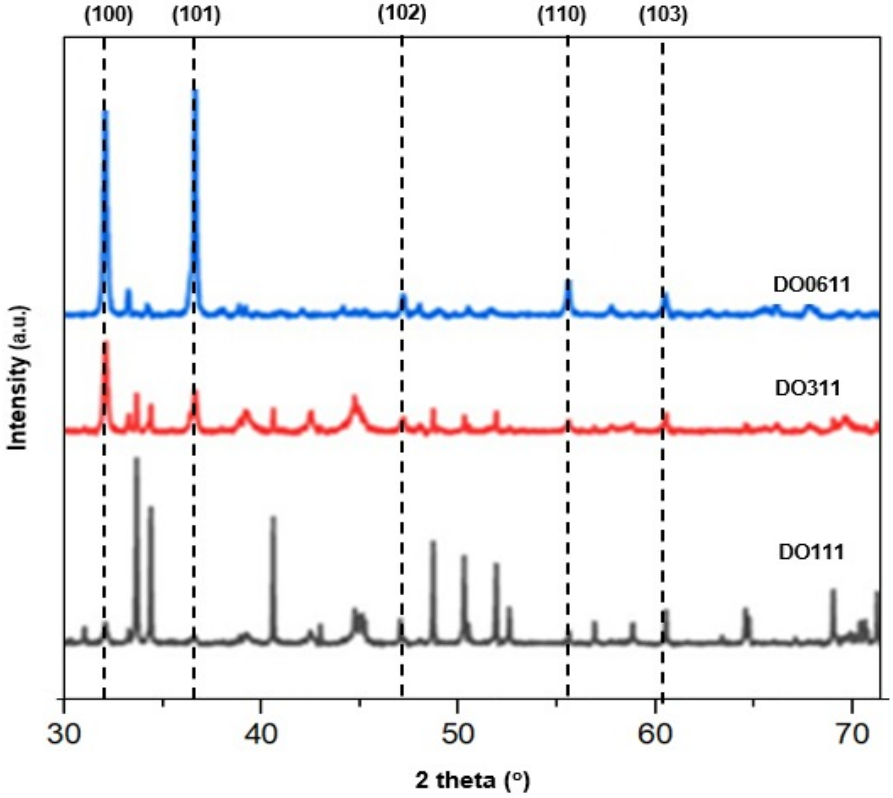

FIGURE 2. XRD diffractogram of synthesized ZnO NPs using *E. bulbosa* extract (DO611, DO311, DO111)

ULTRAVIOLET-VISIBLE SPECTROSCOPY (UV-Vis) ABSORPTION SPECTRA OF ZnO NPs

UV-Vis analysis was used to characterize the absorption spectra of green synthesized ZnO NPs between the wavelength ranges from 200 to 800 nm. The results of synthesized ZnO NPS at different volumes of *E. bulbosa* extract are shown in Figure 3(a). The surface plasmon resonance effect of the UV–Vis spectral analysis provides information on the actual synthesis of metal oxide nanoparticles (Ezealisiji et al. 2019). The synthesised ZnO NPs possessed an adsorption band at range of 300 to 400 nm, confirming the formation of ZnO NPs utilizing *E. bulbosa* extract.

The optical band gap was determined using the Tauc plot, which showed a band gap of ZnO (DO111), ZnO (DO311), and ZnO (DO611) are 3.42 eV, 3.67 eV, and 3.89 eV, respectively (Figure 3(b)). As the volume of the extract increased, the band gap values also enhanced from 3.42 to 3.89 eV. This was reported in previous findings in which the band gap widened when the particle size decreased (Gherbi et al. 2022; Kulkarni et al. 2014). Zinc oxide (ZnO) is an important wide bandgap semiconductor with a direct bandgap of 3.37 eV and a large exciton binding energy of 60 meV. This finding is comparable to observations previously published by Soltanian et al. (2021). According to Chakraborty et al. (2020), the peak in the UV spectrum is caused by the interaction of incoming electromagnetic radiation with a surface plasmon at the contact. Furthermore, the particle size, shape, and reaction media dielectric constant all have an impact on the surface plasmon resonance of ZnO NPs.

CHEMICAL AND FUNCTIONAL GROUPS PRESENT IN THE *E. bulbosa* EXTRACT

FTIR is an analytical technique for identifying the chemical compound and functional group of phytochemical substances present in a sample that may function as a stabilizing, reduction, and capping agent during the synthesis of nanoparticles (Ahmad & Kalra 2020; Vijayakumar et al. 2018). Figure 4 shows the FTIR distribution spectrum of ZnO NPs in the range of 4000

cm^{-1} to 500 cm^{-1}. The peaks around 470 cm^{-1} to 480 cm^{-1} correspond to ZnO NPs. In the figure, the infrared bands which ranged between 3230 cm^{-1} and 3250 cm^{-1} correspond to O-H stretching vibrations from alcohols and phenols whereas the bands obtained between 710 cm^{-1} and 720 cm^{-1} indicate C-H bending in alkene group. On the other hand, the peaks detected around 1020 cm^{-1} to 1030 cm^{-1} represent C-O-C glycosidic linkage and N-H group with aromatic stretching vibrations (Munajad, Subroto & Suwarno 2018). As for the peaks that were below 500 cm^{-1}, these peaks represent polyphenols or flavonoid compounds (Khan, Ware & Shimpi 2021). Based on these findings, the biomolecules in *E. bulbosa* may include alcohols, phenols, alkene, aromatic and flavonoid compounds. The presence of phytochemical substances causes all of the vibration bands. It also helps with the reduction and stability of ZnO NPs.

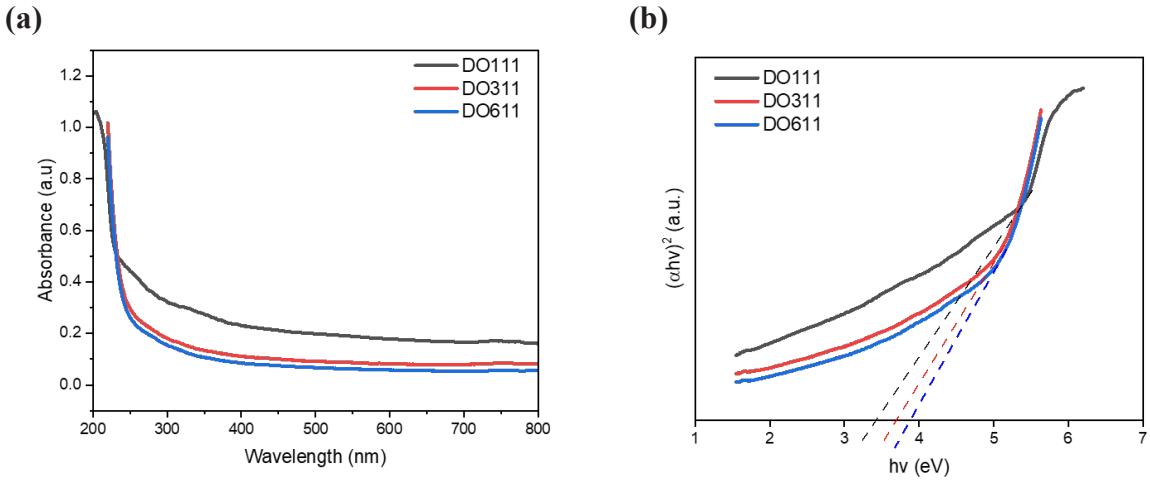

FIGURE 3. (a) UV-Vis spectra of ZnO NPs with different volumes of *E. bulbosa* extract and (b) band gap values of ZnO NPs with different volumes of *E. bulbosa* extract based on plotted graphs of $(\alpha hv)^2$ against photon energy (hυ)

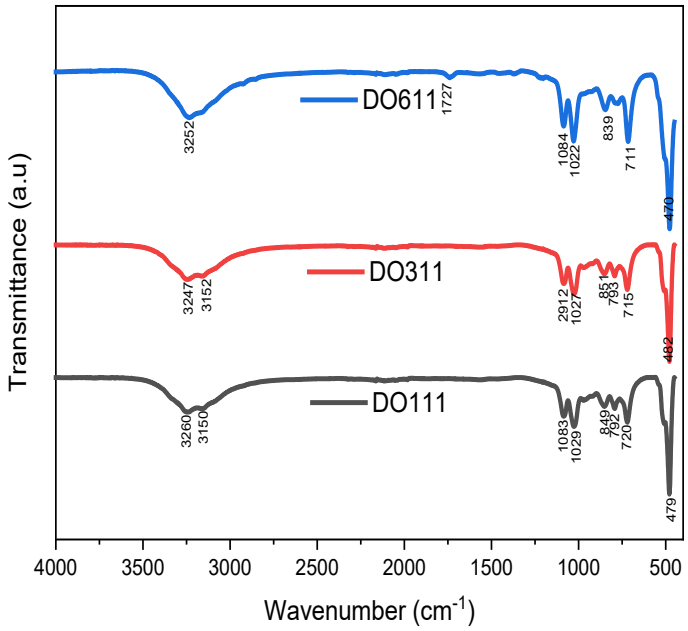

FIGURE 4. The FTIR spectrum of ZnO NPs with different volumes of *E. bulbosa* extract (DO111: 1 mL; DO311: 3 mL; DO611: 6 mL)

PHOTOLUMINESCENCE (PL) SPECTRAL ANALYSIS

The photoluminescence (PL) spectroscopy analysis in Figure 4 shows the purity of ZnO NPs as well as the presence of contaminants like oxygen vacancies (Vo), zinc vacancies (VZn), oxygen interstitials (Oi), zinc interstitials (Zni), and oxygen antisites (OZn). The excitation wavelengths of the synthesized ZnO NPs were found to be within the range of 600-654 nm, as per the photoluminescent spectra. This range indicates the existence of intrinsic defects such as oxygen vacancy (peak 550 nm) and oxygen interstitial (peak 600 nm), with their peaks located at around 550 nm, as per previous findings performed by Markevich et al. (2016) and Mekprasart et al. (2020).

PL spectroscopy is an important approach for investigating the light-emitting capabilities of semiconducting compounds. The PL spectrum of ZnO NPs, synthesized at pH 11 with different extract volumes, is shown in Figure 5. This method was used to confirm the purity and absence of defects in the nanoparticles, as earlier shown by XRD analysis (Vijayakumar et al. 2018). The PL spectra showed that the ZnO NPs have an excitation range of 200 to 800 nm, with significant emission bands observed between 600 and 654 nm. These results are in agreement with previous studies (Markevich et al. 2016). The process of radiative recombination, in which an oxygen vacancy is replaced by a photogenerated hole via the exciton-exciton collision mechanism, explains the peak of visible emission. The red emission is attributed to deep-level emission, caused by intrinsic defects during particle formation and crystal quality in the synthesis process.

ANTIMICROBIAL ACTIVITY AND CYTOTOXICITY OF ZnO NPs

This investigation evaluated the antibacterial effectiveness of ZnO NPs against *S. aureus, E. coli,* and Salmonella, utilizing various volumes of *E. bulbosa* extract and measuring the inhibition zone (Table 2). Overall, it was observed that lower volumes of *E. bulbosa* extract corresponded to greater inhibitory activity against all three bacteria. Furthermore, higher antibacterial activity was observed against the Gram-positive bacteria (*S. aureus*) compared to the Gram-negative bacteria (*E. coli* and Salmonella) for each volume of extract. These results are consistent with a prior study by Imade et al. (2022) which showed that synthesized ZnO NPs have the potential to be an effective therapeutic agent against Gram-positive pathogenic bacteria.

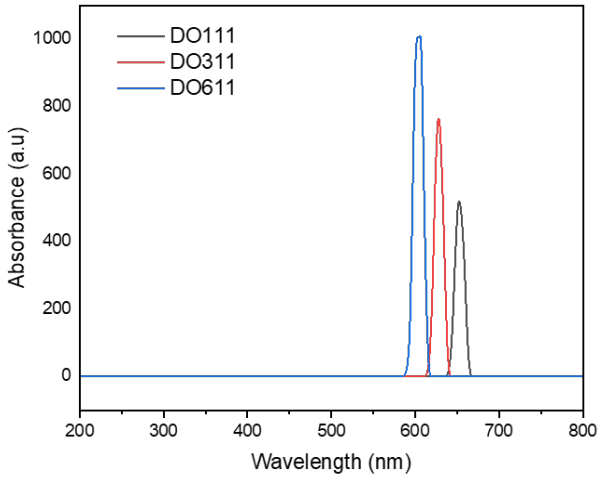

FIGURE 5. Photoluminescence spectra of ZnO NPs using different volumes of *E. bulbosa* extract

TABLE 2. Antimicrobial activity of ZnO NPs *E. bulbosa* extract

Samples	Test strains		
	S. aureus (ATCC43300)	*E. coli* (ATCC25922)	Salmonella (ATCC 10708)
Disk Diffusion Method	The diameter of the disk = 6 mm		
BD611	8.33 mm	7.45 mm	6.98 mm
BD311	7.65 mm	6.75 mm	6.66 mm
BD111	7.32 mm	0	6.6 mm

In contrast to the findings of this investigation, Roy and Rhim (2019) reported that ZnO NPs normally more susceptible to antibacterial activity compared to Gram-positive bacteria because of the natural barrier provided by the cell wall of the latter. The antibacterial activity of ZnO NPs is influenced by factors such as their particle size and concentration. According to Peng et al. (2011), the antibacterial action of ZnO NPs was due to their increased surface area and higher concentration. Because of the increased interfacial area, the smaller size of ZnO NPs allows for improved penetration of bacterial membranes.

As for the cytotoxicity, only ZnO NPs (DO611) were tested against MCF-7 and MCF-10A cells as they showed the most significant characteristic of ZnO NPs. Based on the viability of cells plotted against increasing concentrations of ZnO NPs (DO111), the IC_{50} values for MCF-7 and MCF-10A cells were 2.503 μg/mL and 15.77 μg/mL, respectively (Figure 6(a) and 6(b)). This was consistent with previous studies that described the cytotoxic activity of synthesized ZnO NPs against non-tumorigenic lung WI38 and tumorigenic colorectal

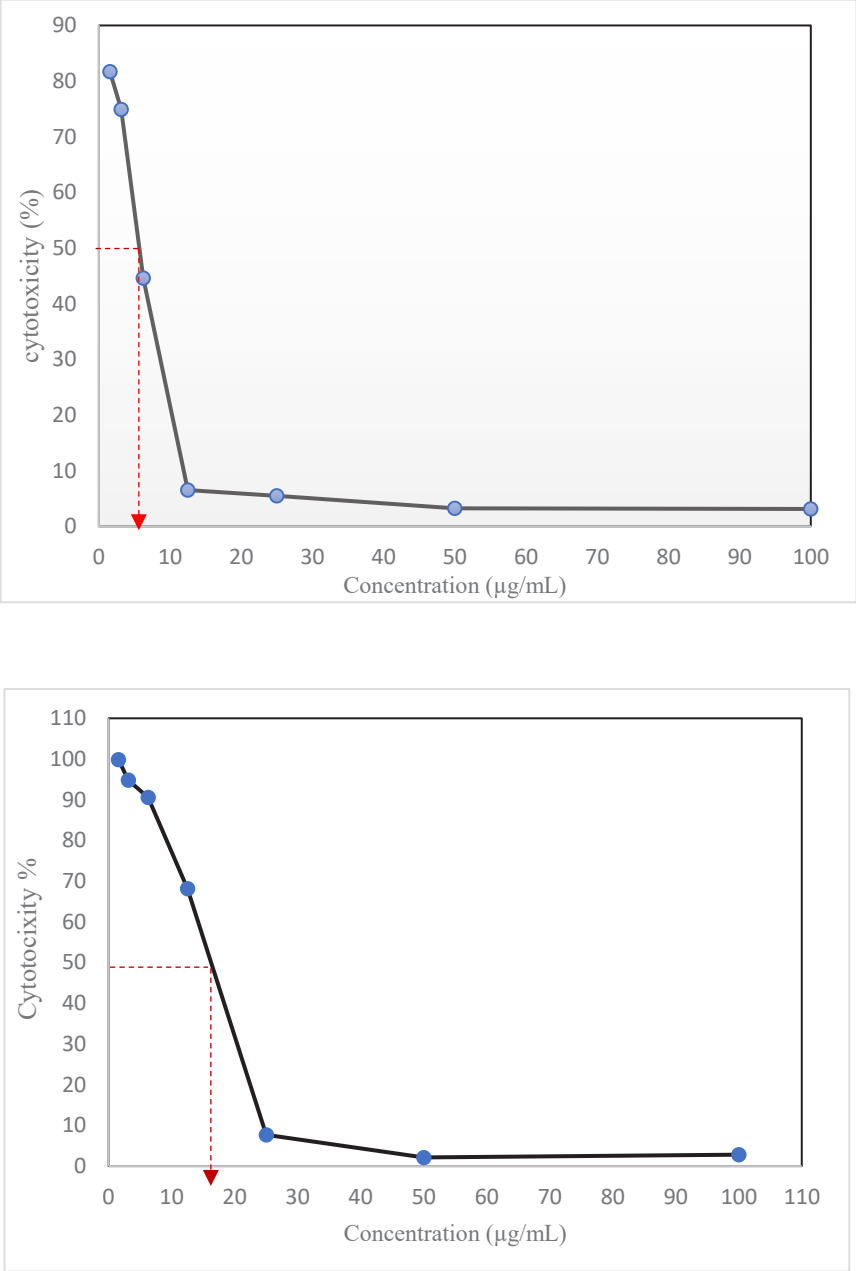

FIGURE 6. The viability of (a) MCF-7 and (b) MCF-10A cells after treatment with different concentrations of ZnO NPs using 1 mL of E. *bulbosa* extract (DO111).

Caco-2 cell lines (El-Belely et al. 2021). The cytotoxic response of ZnO NP samples to cancer cells was dependent on their surface structures and properties. This result explains the properties of positive charge of nanoparticles may have higher cellular uptake due to electrostatic interactions, potentially leading to increased cytotoxicity. Besides, the modification of nanoparticle surfaces with various functional groups or coatings can impact their stability, solubility, and interactions with cells (Altunbek, Baysal & Culha 2014).

Previous research has indicated that ZnO NPs can exhibit selective cytotoxicity against cancerous cell lines while sparing non-tumorigenic cells. For example, ZnO-NPs created using the methanolic extract of *Sargassum muticum* algal species showed toxicity against MCF-7 and MDA-MB-231 human breast cancer cells but not against non-cancerous Vero monkey kidney cells (Namvar et al. 2013). Similarly, Berehu et al. (2021) found that synthesized nanoparticles using ethanol and methanol crude extracts of *S. chirayita* leaves were toxic to HCT-116 and Caco-2 colorectal cancer cells but not to human embryonic kidney cells (HEK-293). However, there is inconsistency in the literature regarding the selective cytotoxicity of ZnO NPs to cancer cells, which could be due to differences in cell lines, methods of synthesis, synthesis parameters, and the types of plants used for synthesis.

Conclusions

In summary, ZnO NPs were successfully synthesized using *E. bulbosa* extract in three different volumes. ZnO nanoparticles (NPs) with 1 mL of *E. bulbosa* bulb extract displays the best characteristics on structural and optical analyses. However, 6 mL of *E. bulbosa* bulb extract showed a better result of the physicochemical properties analysis. This discrepancy in outcomes may be explained by the possibility that smaller concentrations of *E. bulbosa* bulb extract (1 mL) can emphasise or optimise particular qualities, whereas higher quantities (6 mL) might enhance different traits. Therefore, the exact application should be taken into account while selecting the *E. bulbosa* bulb extract volume.

Acknowledgments

This study was funded by Kurita Water and Environment Foundation (21Pmy133-30A). The authors express their gratitude to the management of UPM-MAKNA Cancer Research, Institute of Bioscience, UPM for providing the necessary facilities during the course of this work.

References

Abomuti, M.A., Danish, E.Y., Firoz, A., Hasan, N. & Malik, M.A. 2021. Green synthesis of zinc oxide nanoparticles using *Salvia officinalis* leaf extract and their photocatalytic and antifungal activities. *Biology* 10(11): 1075. https://doi: 10.3390/biology10111075

Agarwal, H., Venkat Kumar, S. & Rajeshkumar, S. 2017. A review on green synthesis of zinc oxide nanoparticles – An eco-friendly approach. *Resource-Efficient Technologies* 3(4): 406-413. https://doi.org/10.1016/j.reffit.2017.03.002

Agasti, N. & Narender, K. Kaushik. 2018. Synthesis and characterization of stearic acid capped silver nanoparticles: pH-dependent stabilization and colorimetric detection of Hg(II) in water. *Advanced Materials Letters* 9(1): 53-57. https://doi.org/10.5185/amlett.2018.1756

Ahmad, W. & Kalra, D. 2020. Green synthesis, characterization and anti microbial activities of ZnO nanoparticles using *Euphorbia hirta* leaf extract. *Journal of King Saud University - Science* 32(4): 2358-2364. https://doi.org/10.1016/j.jksus.2020.03.014

Altunbek, M., Baysal, A. & Culha, M. 2014. Influence of surface properties of zinc oxide nanoparticles on their cytotoxicity. *Colloids and Surfaces* 121: 106-113. https://doi.org/10.1016/j.colsurfb.2014.05.034

Anbuvannan, M., Ramesh, M., Viruthagiri, G., Shanmugam, N. & Kannadasan, N. 2015. *Anisochilus carnosus* leaf extract mediated synthesis of zinc oxide nanoparticles for antibacterial and photocatalytic activities. *Materials Science in Semiconductor Processing* 39: 621-628. https://doi.org/10.1016/j.mssp.2015.06.005

Awwad, A.M., Amer, M.W., Salem, N.M. & Abdeen, A.O. 2020. Green synthesis of zinc oxide nanoparticles (ZnO-NPs) using *Ailanthus altissima* fruit extracts and antibacterial activity. *Chemistry International* 6(3): 151-159.

Bala, N., Saha, S., Chakraborty, M., Maiti, M., Das, S., Basu, R. & Nandy, P. 2015. Green synthesis of zinc oxide nanoparticles using *Hibiscus subdariffa* leaf extract: Effect of temperature on synthesis, anti-bacterial activity and anti-diabetic activity. *RSC Advances* 5(7): 4993-5003. https://doi.org/10.1039/c4ra12784f

Balouiri, M., Sadiki, M. & Ibnsouda, S.K. 2016. Methods for *in vitro* evaluating antimicrobial activity: A review. *Journal of Pharmaceutical Analysis* 6(2): 71-79. https://doi.org/10.1016/j.jpha.2015.11.005

Berehu, H.M., Anupriya, S., Khan, M.I., Chakraborty, R., Lavudi, K., Penchalaneni, J., Mohapatra, B., Mishra, A. & Patnaik, S. 2021. Cytotoxic potential of biogenic zinc oxide nanoparticles synthesized from *Swertia chirayita* leaf extract on colorectal cancer cells. *Frontiers in*

Bioengineering and Biotechnology 9: 788527. https://doi.org/10.3389/fbioe.2021.788527

Chakraborty, U., Bhanjana, G., Adam, J., Mishra, Y.K., Kaur, G., Chaudhary, G.R. & Kaushik, A. 2020. A flower-like ZnO-Ag2O nanocomposite for label and mediator free direct sensing of dinitrotoluene. *RSC Advances* 10(46): 27764-27774. https://doi.org/10.1039/d0ra02826f

El-Belely, E.F., Farag, M.M.S., Said, H.A., Amin, A.S., Azab, E., Gobouri, A.A. & Fouda, A. 2021. Green synthesis of zinc oxide nanoparticles (ZnO-NPs) using *Arthrospira platensis* (Class: Cyanophyceae) and evaluation of their biomedical activities. *Nanomaterials (Basel)* 11(1): 95. https://doi.org/10.3390/nano

Ezealisiji, K.M., Siwe-Noundou, X., Maduelosi, B., Nwachukwu, N. & Krause, R.W.M. 2019. Green synthesis of zinc oxide nanoparticles using Solanum torvum (L) leaf extract and evaluation of the toxicological profile of the ZnO nanoparticles–hydrogel composite in Wistar albino rats. *International Nano Letters* (9): 99–107. https://doi.org/10.1007/s40089-018-0263-1

Gherbi, B., Laouini, S.E., Meneceur, S., Bouafia, A., Hemmami, H., Tedjani, M.L., Thiripuranathar, G., Barhoum, A. & Menaa, F. 2022. Effect of pH value on the bandgap energy and particles size for biosynthesis of ZnO nanoparticles: Efficiency for photocatalytic adsorption of methyl orange. *Sustainability* 14(18): 11300.

Hano, C. & Abbasi, B.H. 2022. Plant-based green synthesis of nanoparticles: Production, characterization and applications. *Biomolecules* 12(1): 1-9. https://doi.org/10.3390/biom12010031

Imade, E.E., Ajiboye, T.O., Fadiji, A.E., Onwudiwe, D.C. & Babalola, O.O. 2022. Green synthesis of zinc oxide nanoparticles using plantain peel extracts and the evaluation of their antibacterial activity. *Scientific African* 16: e01152. https://doi.org/10.1016/j.sciaf.2022.e01152

Insanu, M., Kusmardiyani, S. & Hartati, R. 2014. Recent studies on phytochemicals and pharmacological effects of *Eleutherine Americana* Merr. *Procedia Chemistry* 13: 221-228. https://doi.org/10.1016/j.proche.2014.12.032

Jain, A.S., Pawar, P.S., Sarkar, A., Junnuthula, V. & Dyawanapelly, S. 2021. Bionanofactories for green synthesis of silver nanoparticles: Toward antimicrobial applications. *International Journal of Molecular Sciences* 22(21): 11993. https://doi.org/10.3390/ijms222111993

Kamarudin, A.A., Mohd. Esa, N., Saad, N., Sayuti, N.H. & Nor, N.A. 2020. Heat assisted extraction of phenolic compounds from *Eleutherine bulbosa* (Mill.) bulb and its bioactive profiles using response surface methodology. *Industrial Crops and Products* 144: 112064. https://doi.org/10.1016/j.indcrop.2019.112064

Khan, M., Ware, P. & Shimpi, N. 2021. Synthesis of ZnO nanoparticles using peels of *Passiflora foetida* and study of its activity as an efficient catalyst for the degradation of hazardous organic dye. *SN Applied Sciences* 3(5): 1-17. https://doi.org/10.1007/s42452-021-04436-4

Kulkarni, S.A., Sawadh, P.S., Palei, P.K. & Kokate, K.K. 2014. Effect of synthesis route on the structural, optical and magnetic properties of Fe_3O_4 nanoparticles. *Ceramics International* 40(1 PART B): 1945-1949. https://doi.org/10.1016/j.ceramint.2013.07.103

Kusuma, I.W., Arung, E.T., Rosamah, E., Purwatiningsih, S., Kuspradini, H., Syafrizal, Astuti, J., Kim, Y.U. & Shimizu, K. 2010. Antidermatophyte and antimelanogenesis compound from *Eleutherine americana* grown in Indonesia. *Journal of Natural Medicines* 64(2): 223-226. https://doi.org/10.1007/s11418-010-0396-7

Markevich, I., Stara, T., Khomenkova, L., Kushnirenko, V. & Borkovska, L. 2016. Photoluminescence engineering in polycrystalline ZnO and ZnO-based compounds. *AIMS Materials Science* 3(2): 508-524. https://doi.org/10.3934/matersci.2016.2.508

Mekprasart, W., Ravuri, B.R., Yimnirun, R. & Pecharapa, W. 2020. Photoluminescence and X-ray photoelectron spectroscopic study of milled-ZnO material prepared by high energy ball milling technique. *ScienceAsia* 46 S(1): 91-96. https://doi.org/10.2306/SCIENCEASIA1513-1874.2020.S013

Melkamu, W.W. & Bitew, L.T. 2021. Green synthesis of silver nanoparticles using *Hagenia abyssinica* (*Bruce*) *J.F. Gmel* plant leaf extract and their antibacterial and anti-oxidant activities. *Heliyon* 7(11): e08459. https://doi.org/10.1016/j.heliyon.2021.e08459

Munajad, A., Subroto, C. & Suwarno. 2018. Fourier transform infrared (FTIR) spectroscopy analysis of transformer paper in mineral oil-paper composite insulation under accelerated thermal aging. *Energies* 11(2): 364. https://doi.org/10.3390/en11020364

Namvar, F., Mohamad, R., Baharara, J., Zafar-Balanejad, S., Fargahi, F. & Rahman, H.S. 2013. Antioxidant, antiproliferative, and antiangiogenesis effects of polyphenol-rich seaweed (*Sargassum muticum*). *BioMed Research International* 2013: 604787. https://doi.org/10.1155/2013/604787

Peng, X., Palma, S., Fisher, N.S. & Wong, S.S. 2011. Effect of morphology of ZnO nanostructures on their toxicity to marine algae. *Aquatic Toxicology* 102(3-4): 186-196. https://doi.org/10.1016/j.aquatox.2011.01.014

Pillai, A.M., Sivasankarapillai, V.S., Rahdar, A., Joseph, J., Sadeghfar, F., Anuf, A.R., Rajesh, K. & Kyzas, G.Z. 2020. Green synthesis and characterization of zinc oxide nanoparticles with antibacterial and antifungal activity. *Journal of Molecular Structure* 1211: 128107. https://doi.org/10.1016/j.molstruc.2020.128107

Ribut, S.H., Abdullah, C.A.C., Mustafa, M., Yusoff, M.Z.Y. & Azman, S.N.A. 2018. Influence of pH variations on zinc oxide nanoparticles and their antibacterial activity. *Materials Research Express* 6(2): 025016. http://doi.org/10.1088/2053-1591/aaecbc

Roy, S. & Rhim, J.W. 2019. Carrageenan-based antimicrobial bionanocomposite films incorporated with ZnO nanoparticles stabilized by melanin. *Food Hydrocolloids* 90: 500-507. https://doi.org/10.1016/j.foodhyd.2018.12.056

Selim, Y.A., Azb, M.A., Ragab, I. & H.M. Abd El-Azim, M. 2020. Green synthesis of zinc oxide nanoparticles using aqueous extract of *Deverra tortuosa* and their cytotoxic activities. *Scientific Reports* 10(1): 1-9. https://doi.org/10.1038/s41598-020-60541-1

Siddiqi, K.S., ur Rahman, A., Tajuddin, & Husen, A. 2018. Properties of zinc oxide nanoparticles and their activity against microbes. *Nanoscale Research Letters* 13(1): 141. https://doi.org/10.1186/s11671-018-2532-3

Soltanian, S., Sheikhbahaei, M., Mohamadi, N., Pabarja, A., Abadi, M.F.S. & Tahroudi, M.H.M. 2021. Biosynthesis of zinc oxide nanoparticles using *Hertia intermedia* and evaluation of its cytotoxic and antimicrobial activities. *BioNanoScience* 11(2): 245-255. https://doi.org/10.1007/s12668-020-00816-z

Soto-Robles, C.A., Luque, P.A., Gómez-Gutiérrez, C.M., Nava, O., Vilchis-Nestor, A.R., Lugo-Medina, E., Ranjithkumar, R. & Castro-Beltrán, A. 2019. Study on the effect of the concentration of *Hibiscus sabdariffa* extract on the green synthesis of ZnO nanoparticles. *Results in Physics* 15: 102807. https://doi.org/10.1016/j.rinp.2019.102807

Theophil Anand, G., Renuka, D., Ramesh, R., Anandaraj, L., John Sundaram, S., Ramalingam, G., Magdalane, C.M., Bashir, A.K.H., Maaza, M. & Kaviyarasu, K. 2019. Green synthesis of ZnO nanoparticle using *Prunus dulcis* (Almond Gum) for antimicrobial and supercapacitor applications. *Surfaces and Interfaces* 17: 100376. https://doi.org/10.1016/j.surfin.2019.100376

Van, T.A., Joubert, A.M. & Cromarty, A.D. 2015. Limitations of the 3-(4,5-dimethylthiazol-2-yl)-2,5-diphenyl-2H-tetrazolium bromide (MTT) assay when compared to three commonly used cell enumeration assays. *BMC Res Notes* 8: 47. https://bmcresnotes.biomedcentral.com/articles/10.1186/s13104-015-1000-8

Vijayakumar, S., Mahadevan, S., Arulmozhi, P., Sriram, S. & Praseetha, P.K. 2018. Green synthesis of zinc oxide nanoparticles using *Atalantia monophylla* leaf extracts: Characterization and antimicrobial analysis. *Materials Science in Semiconductor Processing* 82: 39-45. https://doi.org/10.1016/j.mssp.2018.03.017

Wicaksono, I., Runadi, D. & Firmansyah, I. 2018. Antibacterial activity test of dayak onions (*Eleutherine palmifolia* L. Merr.) ethanolic extract against *Shigella dysenteriae* ATCC 13313. *National Journal of Physiology, Pharmacy and Pharmacology* 8(5): 741-744. https://doi.org/10.5455/njppp.2018.8.1248625012018

Zhen, L., Zhang P., Andrea, P., Tobias, K. & Dietrich, A.V. 2020. Influence of core size and capping ligand of gold nanoparticles on the desorption/ionization efficiency of small biomolecules in AP-SALDI-MS. *Analytical Science Advances* (1): 210–220. https://doi.org/10.1002/ansa.202000002

*Corresponding author; email: norazalina@upm.edu.my